PSAMMAPLINS SELECTIVELY TARGET TRIPLE-NEGATIVE METASTATIC
BREAST TUMOR CELLS THAT ARE GENENETICALLY PROGRAMMED TO
COLONIZE SPECIFIC ORGANS

by
Thuy Phuong T. Le

A thesis submitted to the faculty of The University of Mississippi in partial fulfillment of
the requirements of the Sally McDonnell Barksdale Honors College.

Oxford
May 2017

Approved by

_____
Advisor: Professor Yu-Dong Zhou

_____
Reader: Professor Dale George Nagle

_____
Reader: Professor Joseph Rhea Gladden

ACKNOWLEDGMENTS

First of all, I would like to thank Dr. Yu-Dong Zhou and Dr. Dale G. Nagle for listening to my research interests and allowing me to bring them to life. Thank you Dr. Zhou for her expertise, guidance, and support in advising this project. Dr. Zhou was there for me to ease all of my worries throughout this stressful process, and I will forever be grateful for her. Thank you Dr. Nagle for being my second reader and providing me edits for my thesis. Also, thank you to Dr. Nagle's research group for allowing me to contribute to their project.

I would like to give my thanks to Dr. Joseph R. Gladden for serving as my third reader and expressing interest in my thesis.

I would also like to thank the Sally McDonnel Barksdale Honors College, especially Dr. John Samonds, for supporting my career goals and providing me with opportunities that helped me get closer to achieving them.

Finally, I want to express my sincere gratitude to my family, Michelle Ha, and Amber Vu for providing me with immense support and encouragement throughout my time at the University of Mississippi and through the process of researching and writing this thesis.

ABSTRACT

THUY PHUONG THI LE: Psammaplins Selectively Target Triple-Negative Metastatic Breast Tumor Cells that are Genetically Programmed to Colonize Specific Organs
(Under the direction of Dr. Yu-Dong Zhou)

Five bromotyrosine-derived marine sponge metabolites, four psammaplins (**1 – 4**) and the psammaplin dimer, bisaprasin (**5**) were isolated from a lipid extract sample of the marine sponge *Dendrilla lacunosa.* Psammaplins act as histone deacetylase (HDAC) inhibitors that alter cellular gene expression. The *D. lacunosa* psammaplins activated the oxygen regulated transcription factor HIF-1 (hypoxia-inducible factor-1) in T47D human breast tumor cells and displayed cell line specific effects against aggressive organotropic metastatic cell lines that were derived from triple-negative MDA-MB-231 human breast tumor cells.

TABLE OF CONTENTS

LIST OF FIGURES

Chapter 1

Introduction

Thuy Phuong T. Le

1.1 Breast Cancer Background

Aside from skin cancers, breast cancer is the most prevalent cancer among women in the United States. Breast cancer affects about one in eight women, and there are varying factors including socioeconomic status, age, race/ethnicity, and geography[1]. Breast cancer is characterized by a mass of cells that originates in the tissues of the breast, and there are many processes involved leading up to its eventual diagnosis[2]. Six processes have been described as the hallmarks of cancer that include: cells replicating uncontrollably, masses of cells creating capillary networks, cells resisting apoptosis, genes mutating to increase proliferation signals, cells dodging the effects of tumor suppressors, and cells invading into other tissues[3].

According to the American Cancer Society (2017), the prevalence of breast cancer has caused scientists to develop various treatment options[4]. In historical terms, treatment options have transitioned from surgical removal to "precision medicine." Depending on the localization or stage of the breast cancer, treatment options may vary.

1

For localized early stage breast cancer, surgery with a combination of radiation therapy is often used. It is common that a surgical option is combined with other alternatives. In more advanced breast cancer that has metastasized, the patient may be treated with hormone therapy, chemotherapy, or targeted therapy[4]. Targeted drugs that are currently being used to treat breast cancer can work through multiple mechanisms: monoclonal antibody (Trastuzumab, Pertuzumab, Ado-trastuzumab emtansine), kinase inhibitor (Lapatinib), estrogen receptor blockers (Tamoxifen, Fulvestrant), and aromatase inhibitors (Letrozole, Anastrozole, and Examestane)[4]. The impact of these molecular-targeted drugs has been significant, but their use is often not sufficient for complete cures. The multiple hit hypothesis may explain for the resistance of tumor cells to treatment or for reoccurring tumors[5].

1.2 Metastasis

Unfortunately, metastasis is common in most cancers and contributes to 90% of breast cancer deaths. Metastasis occurs when the tumor cells become abnormally invasive, and metastasis is characterized by decreased cell-to-cell adhesion, decreased cell-matrix, digestion of underlying matrix, and transition into a "migratory" phenotype[6]. Another name for metastatic breast cancer is stage IV breast cancer or systemic breast cancer. Metastatic tumors commonly travel to organs that are permissive such as the bone, liver, lung, and brain. For breast cancer, tumor cells tend to metastasize to the bones, brain, and lung. Almost eighty percent of metastatic breast cancer becomes bone metastasis[7]. Brain metastases takes second place as the most common site for metastatic breast cancer, between 20% and 40%[8]. Because of the invasiveness of metastatic tumors, they are extremely difficult to treat and control.

1.3 HDAC inhibitors

Histone deacetylases (HDACs) regulate transcription by removing acetyl groups from the lysine residues of histones and making a gene inactive for expression. HDACs have been associated with a large number of oncogenes and tumor-suppressor genes, and they play a role in developing malignant tumors[9,10]. The majority of HDACs are categorized into two main classes, class I HDACs and class II HDACs. Class I HDACs are localized specifically in the nucleus, while class II HDACs are able to move in and out of the nucleus to the cytoplasm. Class I HDACs consists of HDAC 1, 2, 3, and 8, while class II HDACs has HDAC 4, 5, 6, 7, 9a, 9b, 9c, and 10. More recently, a new class of HDACs (class III HDACs) have been characterized that includes the HDACs, called Sirtuins or SIRT1-7, that are localized in the nucleus, cytoplasm, and mitochondria. HDAC 11 has been recently detected and is not classified as Class IV HDACs[11].

Several HDACs inhibit the function of the p53 tumor-suppressor gene, which contributes to the growth of many tumors[12,14]. An overexpression of HDACs have been used as one of the biomarkers for many cancers including prostate, breast and colon cancer. HDAC inhibitors (HDIs) have the potential to serve as possible therapeutic options for various cancers by reversing HDAC-mediated gene suppression. With the various families of HDACs, HDAC inhibitors are structurally classified into four groups that include hydroxamates, cyclic peptides, alipathic acids, and benzamides[12,13].

The HDIs function by inducing apoptosis, cell cycle arrest, and differentiation in tumor cells, and halting the transformation of normal cells into cancer cell. Vorinostat, Romidepsin, and Panobinostat are HDIs currently used clinically. Vorinostat or suberoylanilide hydroxamic acid (SAHA) (Figure 1) is a drug that falls into the

hydroxomate category of HDAC inhibitors[15]. SAHA is a pan-selective inhibitor (IC_{50} 10

nM) that targets Class I and Class II HDACs[16,19]. The FDA-approved drug Vorinostat is

currently prescribed to those who are affected by cutaneous T-cell lymphoma (CTCL) to

stimulate cancer cell apoptosis[17]. The combination of carfilzomib, a proteasome inhibitor,

and Vorinostat produces a dramatic antitumor effect in a xenograft model and human

primary T-cell lymphoma cells, and the combination is currently in various phase I

clinical trials[18]. Even though Vorinostat has a promising future in pharmacology, it

produces a significant number of side effects, including diarrhea, nausea, extreme fatigue,

hair loss, dry mouth, and muscle aches[17].
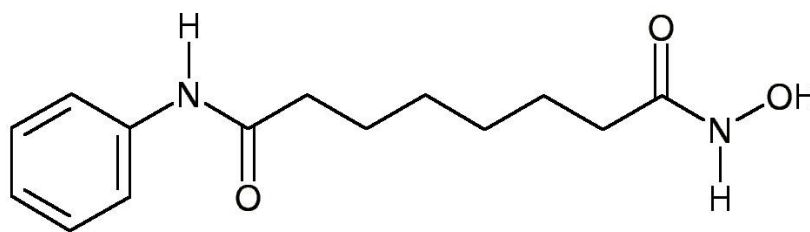
Figure 1. *Chemical Structure of Vorinostat*

Vorinostat can bind to Zn^{+2} and chelate the ion in the active binding site of HDACs[20,21].

Romidepsin is a FDA-approved pan-selective cyclic peptide HDAC inhibitor that

targets Class I HDACs and is effective against CTCL. Following intravenous

administration, romidepsin decreases the rate of cancer cell proliferation and the

induction of the p53/p21 signaling cascades[22,23]. According to *clincaltrials.gov* on March

21, 2017, Romidepsin inhibits both HDAC1 and HDAC2 (IC_{50} 36 nM and 47 nM,

respectively). Compared to other HDAC inhibitors, the potency of romidpesin is

relatively low. Romidepsin combinations with other compounds such as oral 5-

azacitidine, cisplatin, prelatraxate, and many more are actively involved in 31 clinical

trials according to *clinicaltrials.gov* on March 26, 2016. Romedpsin side effects include nausea, diarrhea, constipation, changes taste, and itching[24].
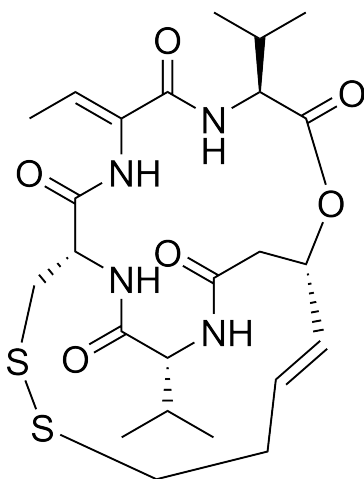
Figure 2. *Chemical Structure of Romidepsin (FK228)*

The HDIs have shown success in stabilizing cutaneous T-cell lymphoma by various mechanisms that include inducing cell arrest and apoptosis. There are current studies that have the purpose to increase the effectiveness of FDA-approved HDIs by creating isoforms or pairing them with other drugs. With the discovery of the effects of HDIs, researchers can develop more specific approaches toward tumor HDACs. The HDIs also show promising potential in treating other diseases and cancers.

1.4 Conclusions

With its high prevalence in women, considerable effort has been placed on the study of breast cancer. Many recently developed drugs do not dramatically improve long-term survival rates. Just as with other cancers, breast cancer can progress into a fatal metastatic form, and it commonly does. Recently developed HDAC inhibitors have unique mechanisms that show great potential as new antitumor drug therapies.

Chapter 2

Psammaplins Selectively Target Triple-Negative Metastatic Breast Tumor Cells that are Genetically Programmed to Colonize Specific Organs

Yu-Dong Zhou, Jun Li, Lin Du, Fakhri Mahdi, **Thuy Phuong T. Le**, Wei-Lun Chen, Steven M. Swanson, and Dale G. Nagle

TPL performed cell viability experiments and analyzed data

1. Introduction

Oxygen homeostasis is considered one of the critical principles in evolution, biology, and medicine. Multicellular organisms have evolved tightly regulated oxygen delivery systems to ensure oxygen dependent energy production. In the human body, high levels of oxygen (hyperoxia) can cause oxygen toxicity and low oxygen levels (hypoxia) are associated with hypoxia-related diseases such as ischemic and neoplastic disorders[25]. At the cellular level, oxygen fluctuations can trigger responses from a network of signaling pathways that modify the gene expression landscape[26,27,28]. Master regulators of oxygen homeostasis, hypoxia-inducible factors (HIFs) are transcription factors that mount cellular responses to hypoxia at the transcription level[29]. Over 100 genes have been

identified as HIF target genes that encode proteins involved in many aspects of cellular physiology, ranging from cellular metabolism, proliferation/survival/death, cytoskeletal structure, adhesion/motility, angiogenesis, erythropoiesis, vascular tone, stemness, to drug resistance[30,31]. Small molecule chemicals that activate HIFs represent potential drug leads for hypoxia-associated diseases and chemical probes for HIF biology and oxygen homeostasis. In fact, a number of HIF-1 activators [e.g., FG-2216 and FG-4592 (FibroGen), GSK1278863 (GlaxoSmithKline), BAY85-3934 (Bayer), and AKB-6548 (Akebia Therapeutics)] are undergoing clinical trials for preventing and alleviating ischemia/reperfusion injuries[32,33,34]. However, most HIF-1 activators target the prolyl hydroxylases that regulate HIF-1α protein stability. Given the complexity of oxygen homeostasis, it is a logical extension to speculate the existence of chemically diverse small molecules that activate HIF-1 through a wide range of pathway(s) and mechanism(s). In a discovery campaign for novel natural product-derived HIF-1 activators, lipid extracts of the sponge *Dendrilla lacunosa* activated HIF-1 in a T47D cell-based reporter assay[35]. Bioassay-guided isolation and chemical structure elucidation afforded five bromotyrosine-derived compounds: four psammaplins and bisaprasin. This study described the characterization of these compounds or HIF-1 activation-associated activities in cell-based in vitro models.

Psammaplins have exhibited a range of bioactivities. Their cytotoxic and/or antitumor activities have been primarily attributed to the inhibition of histone deacetylases (HDACs)[36,37,38,39]. In this study, psammaplins were examined for the ability to suppress organotropic metastatic breast cancers. Systemic metastasis-associated disease relapse accounts for over 90% of cancer mortality. The five-year survival rate is
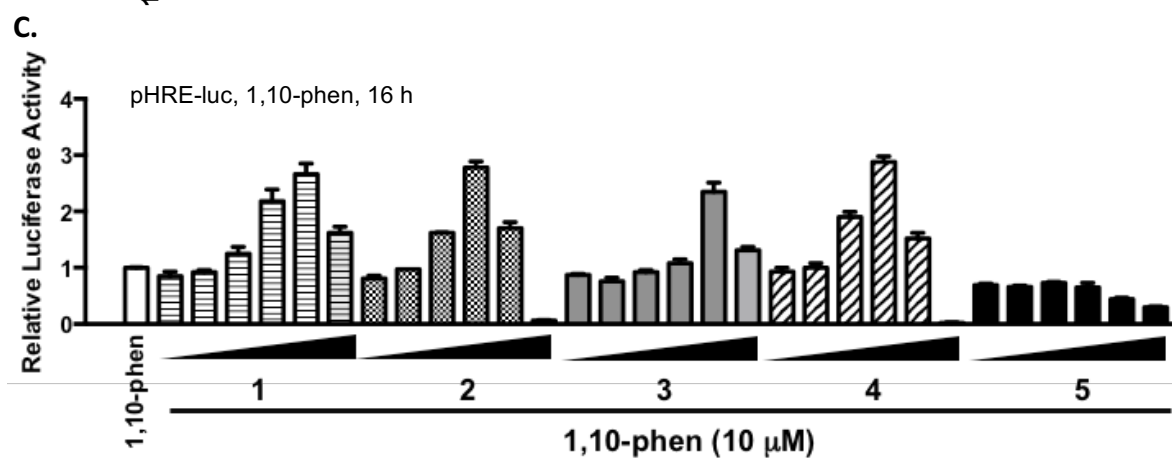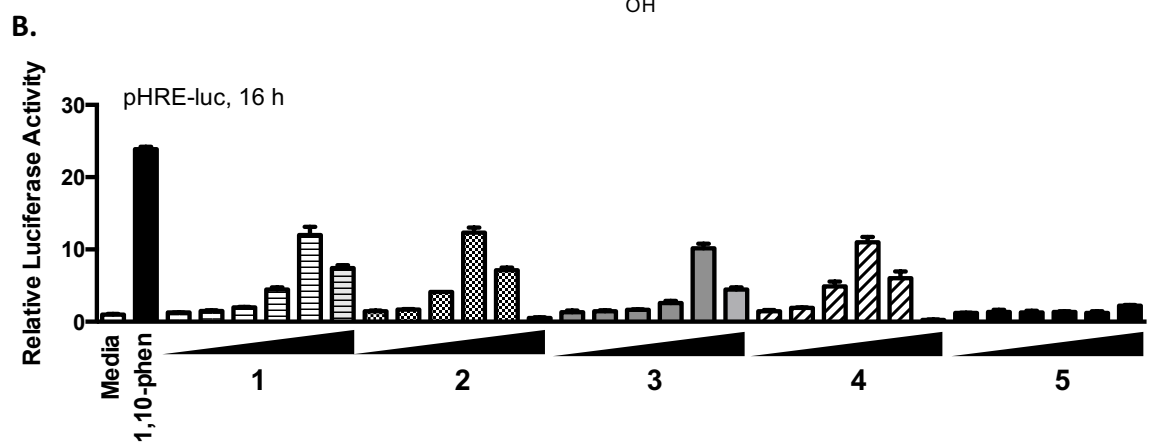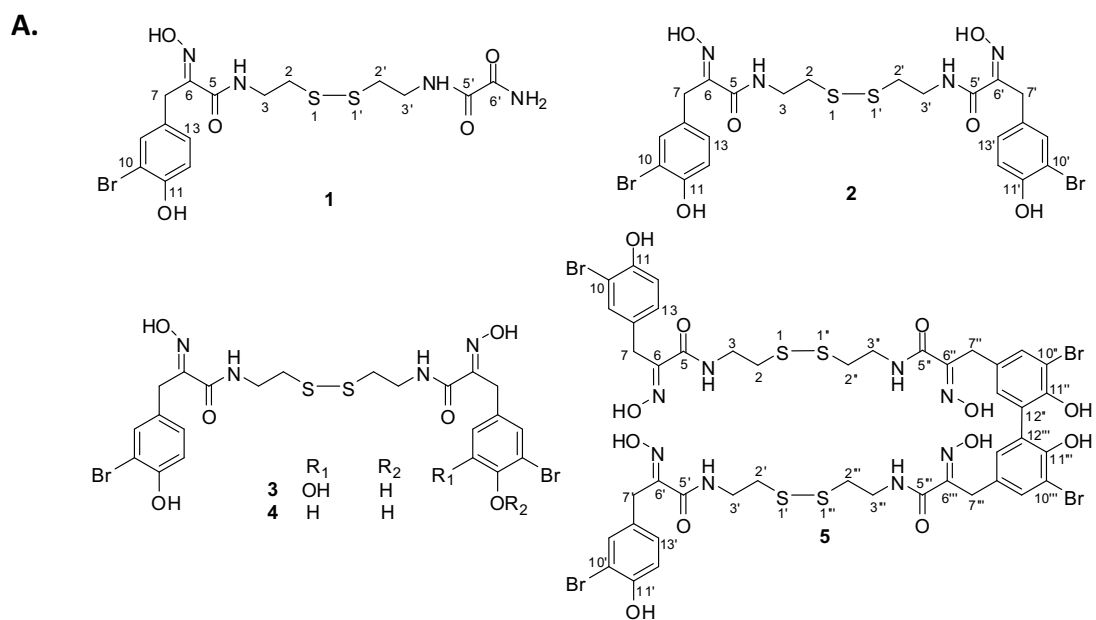
23% among the 162,000 American women with metastatic breast cancer[40]. Breast

cancers can metastasize to multiple organs (i.e., lung, bone, brain, liver, etc.). Employing

the widely studied triple-negative breast cancer (TNBC) cell line MDA-MB-231 as a

model system, the Massagué group isolated organotropic subclones and identified

signature gene expression profiles for lung-, bone-, and brain-specific breast cancer

metastases[41,42,43]. Employing these recently established and genetically characterized

MDA-MB-231 derived organotropic subclones as in vitro models, psammaplins were

examined for the ability to selectively suppress metastatic breast cancer cells in a target

organ-dependent manner. Psammaplins exerted more pronounced inhibitory effects

towards the metastatic subclones specific to bone, in comparison to the others. Herein,

the activities of psammaplins and bisaprasin towards organotropic metastatic breast

cancer cells are described.

2. Results

2.1. Psammaplins Exhibit Concentration-Dependent Biphasic Effects on HIF-1 Activity

In a T47D cell-based reporter assay[34], a lipid extract sample of the sponge

Dendrilla lacunosa activated HIF-1 by 3.56-fold (NIH collection no. C025691, 10 μg

mL^{-1}). Bioassay-guided fractionation of the extract sample (2.6 g) and chemical

structure elucidation afforded five known compounds psammaplin E (**1**), (*E,Z*)-

psammaplin A (**2**), (*E,E*)-psammaplin K (**3**), (*E,E*)-psammaplin A (**4**), and bisaprasin (**5**).

The structures are shown in Figure 3A. To determine the effects of **1–5** on HIF-1

activity, concentration-response studies were performed in a T47D cell-based reporter assay (Figure 3B). An iron chelator (1,10-phenanthroline, 10 μM) was included as a positive control. Compounds **1–4** activated HIF-1 in a biphasic manner. The highest level of activation was observed at the concentrations of 3 μM for **2** and **4** (12.32 ± 0.70 and 11.01 ± 0.71 fold, respectively, *n*=3) and 10 μM for **1** and **3** (12.01 ± 1.12 and 10.15 ± 0.66 fold, respectively, *n*=3). Compound **5** displayed weak HIF-1 activation at 30 μM (2.17 ± 0.13 fold, *n*=3). Hypoxia (1% O_2) and chemical hypoxia (iron chelators or transition metals) represent two common stimuli that activate HIF-1[44]. Further studies were performed to determine the effects of **1–5** on HIF-1 activity in the presence of other stimuli (1,10-phenanthroline, Figure 3C; hypoxia, Figure 3D). While **1–4** acted synergistically with 1,10-phenanthroline and hypoxia inducing HIF-1 activity, a biphasic pattern of activation similar to that in the absence of stimulus (Figure 3A) was observed. In contrast, **5** inhibited HIF-1 activation at higher concentrations. Previous studies reported that psammaplins inhibit histone deacetylase (HDAC)[45]. To determine if HDAC inhibition non-specifically activates HIF-1, concentration-response studies were conducted in T47D cells transfected with the pGL3-control plasmid. As shown in Figure 3E, **1–4** did enhance luciferase activity in T47D cells transfected with the control plasmid. However, the activation of HIF-1 was more pronounced than that of the pGL3-control (e.g., normalized ratio of pHRE-luc/pGL3-control at 2.64 for **1** at 10 μM, 2.38 for **2** at 3 μM, 2.38 for **3** at 10 μM, and 2.30 for **4** at 3 μM). These observations suggest that **1–4** activated HIF-1 with a certain degree of specificity.

A.

B.

pHRE-luc, 16 h

Relative Luciferase Activity

Media
1,10-phen

1   2   3   4   5

C.

pHRE-luc, 1,10-phen, 16 h

Relative Luciferase Activity

1,10-phen

1   2   3   4   5

1,10-phen (10 µM)

D.

E.
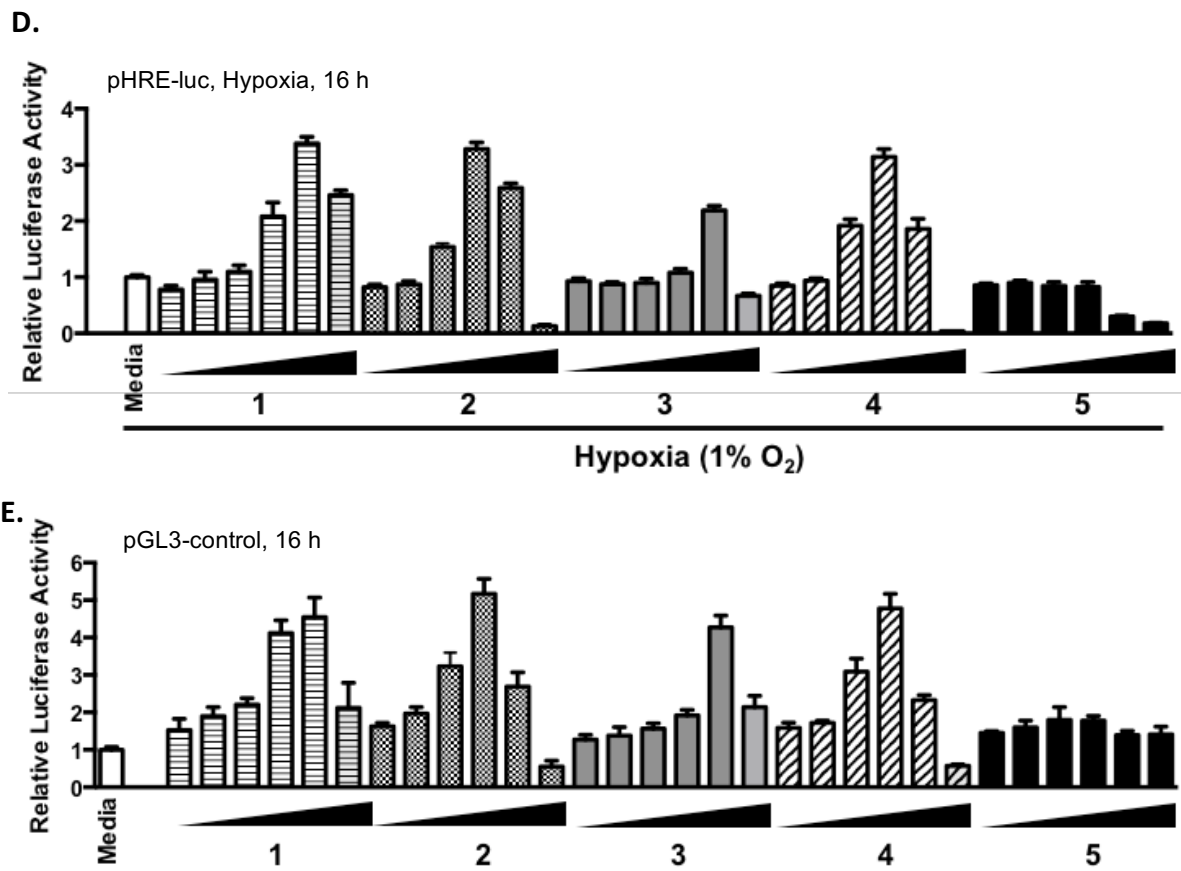
Figure 3. Concentration-dependent biphasic effects of 1–4 on HIF-1 activation. (A) Structures of psammaplins isolated from *Dendrilla lacunosa*. (B) Concentration-response results of **1–5** in T47D cells transfected with pHRE-luc for HIF-1 activity. Test compounds were added at the increasing concentrations of 0.1, 0.3, 1, 3, 10, and 30 μM, as specified. The positive control 1,10-phenanthroline (1,10-phen) was used at 10 μM. Data shown are average ± standard deviation (n = 3). (C) Similar to described in (B) except that the pHRE-luc transfected T47D cells were exposed to test compounds in the presence of 10 μM 1,10-phen, and the data were normalized to the positive control (1,10-phen). (D) Similar to described in (C) except that hypoxic exposure (1% O_2: 5% CO_2: 94% N_2, 16 h) was applied in place of 1,10-phen. (E) As described in (B) except that T47D cells were transfected with the pGL3-control construct.

2.2. Differential HDAC Inhibition by Psammaplin Analogues

The effects of **1–5** on HDAC activity were determined in a human melanoma MDA-MB-435 cell-based assay. Test compounds were added at specified concentrations to exponentially grown cells plated in 96-well plates. After 30 min incubation, the HDAC activity was determined using a commercial kit (HDAC-Glo™) and normalized to that of the solvent control (DMSO). The standard HDAC inhibitors trichostatin A (TSA, 1 nM) and SAHA (100 nM) were included as positive controls. In the MDA-MB-435 cell-based assay, TSA and SAHA inhibited HDAC by 52% ± 8% and 60% ± 5%, respectively (average ± SE, $n = 6$). The IC_{50} values for **1–5** to inhibit HDAC are summarized in Table 1. Compound **2** was the most potent HDAC inhibitor (IC_{50} 0.019 µM), while **5** (IC_{50} 0.948 µM) was the least active.

Table 1. IC_{50} values of **1–5** in a MDA-MB-435 cell-based HDAC assay.

Compound	IC_{50} (µM)	95% CI (µM)[1]
1	0.257	0.157 – 0.420
2	0.019	0.012 – 0.028
3	0.038	0.024 – 0.061
4	0.037	0.025 – 0.055
5	0.948	0.586 – 1.532

[1]Data from two independent experiments ($n = 6$) were pooled to calculate IC_{50}. The 95% confidence interval (95% CI) IC_{50} values are also provided.

2.3. Effects of Psammaplin A on HIF-1 Target Gene Expression

Over 100 genes have been identified as HIF-1 target genes that encode proteins involved in various aspects of cellular physiology. While most of these genes are regulated in a cell type-specific manner, some are induced upon HIF-1 activation in most cell types. Based on the availability and potency, compound **4** was selected for follow-up

studies. The effects of **4** on the expression of HIF-1 target genes *CDKN1A* and *VEGF*
were examined by quantitative real time RT-PCR (Figure 4). The HIF-1 activator 1,10-
phen (10 μM) and the pan-HDAC inhibitor TSA (0.1 and 1 μM) were included as
positive controls. In T47D cells, **4** and TSA each increased the levels of CDKN1A
mRNA in a concentration-dependent manner (2.9-fold for **4** at 10 μM and 7.2-fold for
TSA at 1 μM, Figure 4A). In contrast, neither **4** nor TSA exerted greater than 20% effect
on the levels of VEGF mRNA (Figure 4B). The gene VEGF encodes vascular
endothelial growth factor (a potent angiogenic factor) and agents that inhibit VEGF are in
clinical use for cancer[46]. The expression of cellular and secreted VEGF proteins was
examined in T47D cells by ELISA assay. As anticipated, the positive control 1,10-phen
induced VEGF expression at the levels of mRNA (Figure 4B), cellular protein (Figure
4C), and secreted protein (Figure 4D). None of the HDAC inhibitors examined (**4** and
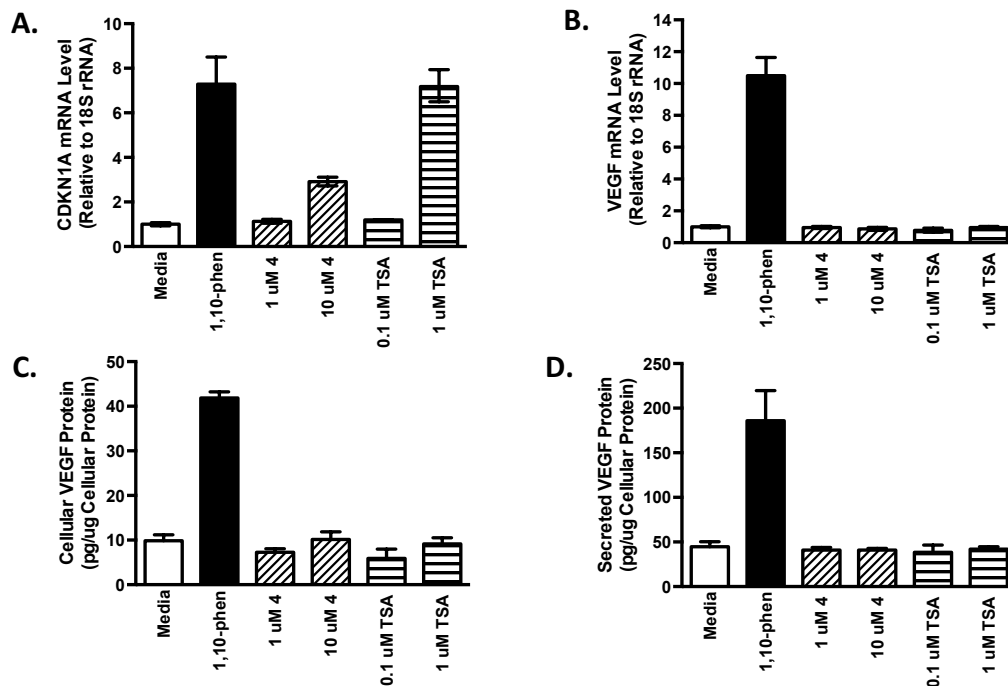TSA) increased VEGF protein levels at the concentrations tested (Figures 4C, 4D).

Figure 4. Effects of 4 and TSA on HIF-1 target gene expression. T47D cells were exposed to **4** and TSA at the specified concentrations for 16 h. The compound 1,10-phen (10 μM) was included as a positive control. The levels of CDKN1A (A) and VEGF (B) mRNA following treatments were determined by quantitative real time RT-PCR. Relative levels of target gene mRNA normalized to an internal control (18S rRNA) are shown as average ± standard deviation (*n*=3, one representative experiment). The levels of cellular (C) and secreted VEGF protein (D) were determined by ELISA and normalized to the amount of cellular proteins. Data shown are average + standard deviation (*n*=3).

2.4. Psammaplins Suppress Cell Proliferation/Viability in a Cell Line-Dependent Manner

In the T47D cell-based reporter assay, psammaplins regulated HIF-1 activity in a biphasic manner (Figure 3). To discern if cytotoxicity contributed to the drop in HIF-1 activity at higher concentrations, the effects of psammaplins on cell proliferation/viability were examined in a panel of established human breast cancer cell lines. The protein synthesis inhibitor cycloheximide (CHX, 10 μM) was used as a positive control and the pan-HDAC inhibitor TSA was included for comparison. Following 48 h of compound treatment, all compounds affected cell proliferation/viability to a certain extent. Among the psammaplins, the potency rank of **2** and **4** > **3** > **1** > **5** mirrored that observed in the HDAC assay (Table 1). Greater inhibitory activity was observed in the triple negative breast cancer (TNBC) MDA-MB-231, MDA-MB-231-derived bone metastatic BoM1833 (BoM) and lung metastatic LM4175 (LM) subclones, and the estrogen-dependent T47D cells, in comparison to the MDA-MB-231-derived brain metastatic subclone BrM-2a

(BrM) (Figure 5). Similar cell line-dependent inhibitory activity was observed with TSA (Figure 5).

A. T47D

B. MDA-MB-231

C. MDA-MB-231-derived subclone LM4175

D. MDA-MB-231-derived subclone BoM1833

E. MDA-MB-231-derived subclone BrM-2a
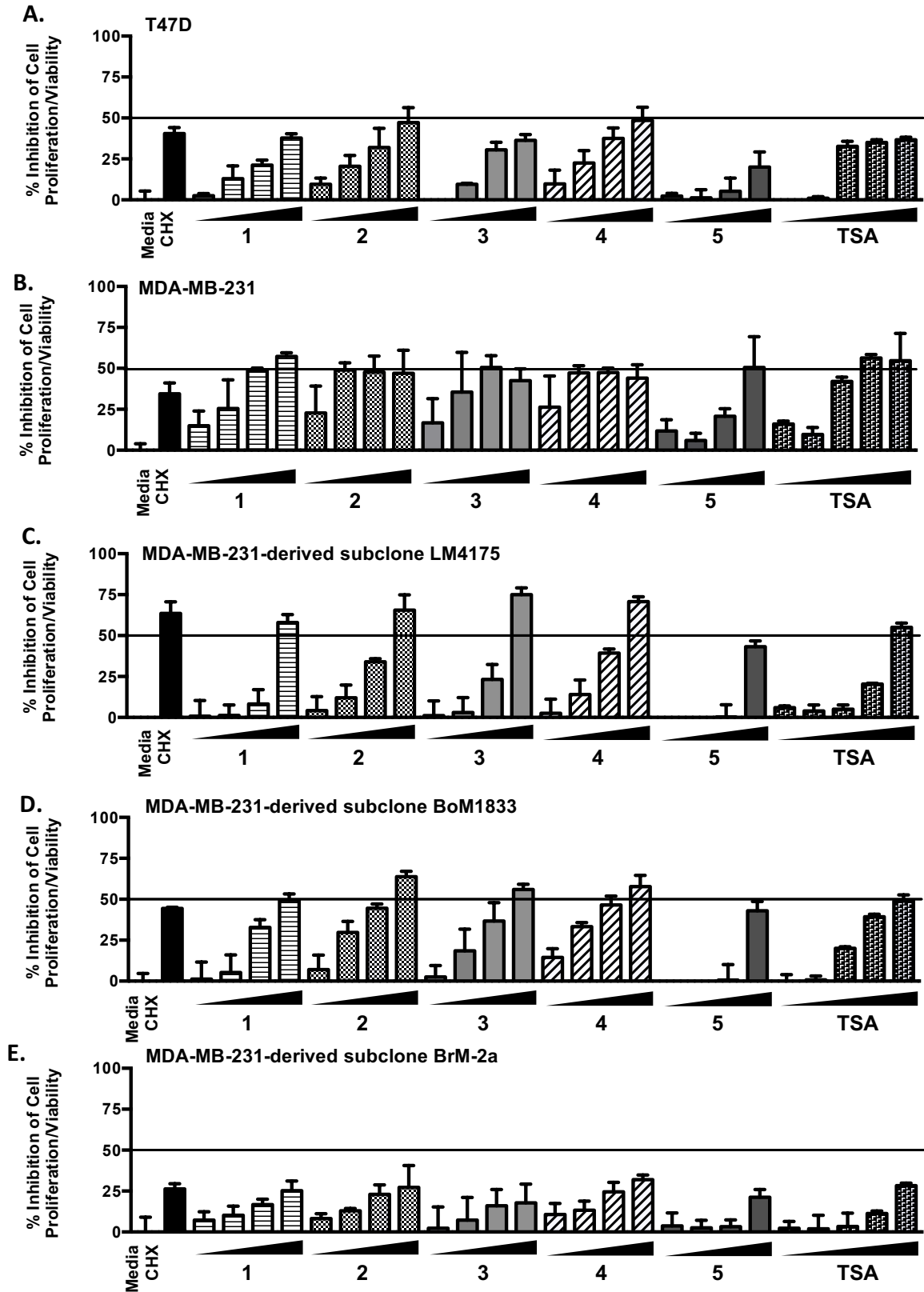
Figure 5. Concentration-response results of 1–5 and TSA on cell proliferation/ viability. T47D (A), MDA-MB-231 (B), LM (C), BoM (D), and BrM (E) cells were exposed to **1–5** at the concentrations of 1, 3, 10, and 30 μM, TSA at 0.01, 0.03, 0.1, 0.3, and 1 μM, and CHX at 10 μM. After 48 h, cell viability was determined and presented as "% Inhibition" of the media control. Data shown are average + standard deviation, pooled from two experiments each performed in duplicate.

The effects of psammaplins on the colony-forming ability of single cells were assessed in a clonogenic assay. Cells seeded at low density were exposed to test compounds at the specified concentrations for 24 h. The conditioned media were replaced with growth media and the colonies formed from single cells in 14 days. While the cell lines differ in their colony-forming abilities, the positive control paclitaxel blocked colony formation in all cell lines (Figure 6). Less pronounced colony-suppressing activity was observed with the HDAC inhibitors.

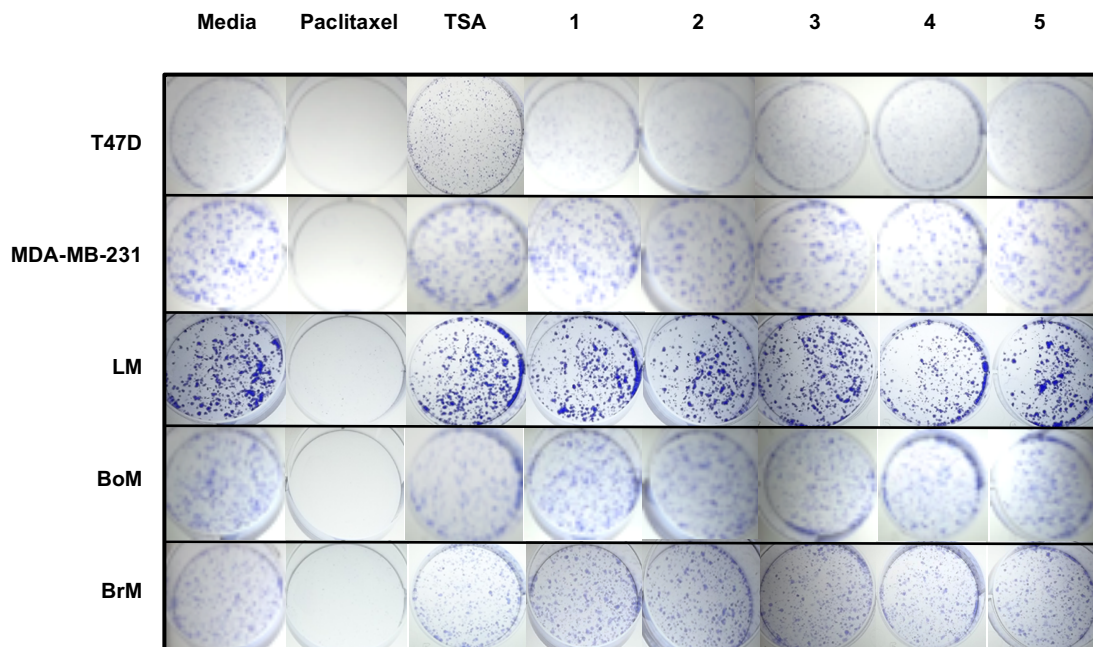**Figure 6. Effects of 1–5 and TSA on colony formation.** Cells plated at low density were exposed to compounds (24 h) at specified concentrations (1 μM for paclitaxel and TSA, and 10 μM for **1–5**). Two weeks later, the cells were fixed and stained.

2.5. Psammaplin A and TSA Inhibit Tumor Cell Invasion

In order to form metastatic lesions, metastasis-initiating tumor cells must invade and intravasate into the lymphatic vasculature and/or blood vessels. Psammaplins were evaluated in a Cultrex® 3-D cell invasion assay that monitors the invasion and migration of tumor cells grown as spheroids, which closely model *in vivo* pathophysiological conditions. The bone metastatic BoM subclone displayed the most aggressive behavior (a network of extensive projections from the spheroid, Figure 7). Compound **4** and TSA each inhibited the invasion of BoM spheroids into the extracellular matrix (ECM), similar to those observed in the presence of the positive controls paclitaxel and CHX (Figure 7). Furthermore, a more pronounced decrease in the size of the spheroids was observed in the presence of paclitaxel and CHX, in comparison to the HDAC inhibitors.
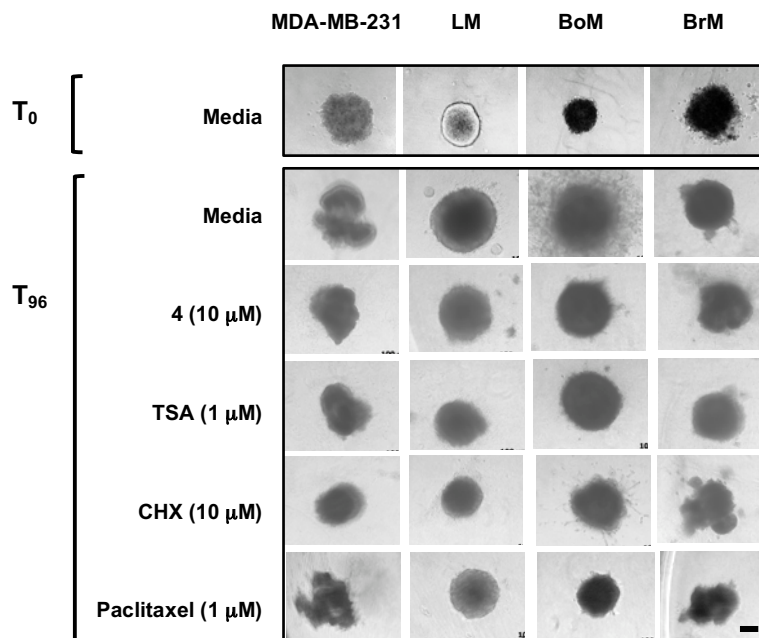
Figure 7. Inhibition of bone metastatic BoM cell invasion. Tumor cell spheroids formed in a special spheroid formation ECM were embedded in an invasion matrix containing 10% FBS in the presence and absence of compounds at the specified concentrations. Four days later (T_{96}), cell invasion was recorded microscopically (the bar at the bottom right represents 100 μm).

3. Discussion

Prevention and improved therapies have produced a steady decline in cancer rates in developed countries[47]. In spite of this success, systemic metastasis-associated disease relapse accounts for over 90% of cancer mortality. Targeted therapies have limited success in stalling cancer progression and improving overall survival. Even highly responsive tumors often develop resistance by acquiring new mutations or by activating complimentary signaling pathways within a few months of treatment. Currently, there is still no treatment option that effectively curbs the spread of cancers to vital organs[48,49].

The century-old "seed and soil" hypothesis of cancer metastasis compares systemically distributed tumor cells to "seeds," and selected organs colonized by disseminated tumor cells as "soil." Metastasis-initiating tumor cells invade and intravasate into the lymphatic vasculature and/or blood vessels, survive the circulation, extravasate to distant target organs, adapt to the new environment, and progress from dormancy to outgrowth into secondary lesions[48]. The inherent complexity of metastatic disease and technological limitations has hindered our molecular level understanding of metastasis and, subsequently, the discovery of antimetastatic agents. Treatment options for metastatic breast cancer include surgery, radiation, chemotherapy, hormones, and molecular-targeted therapies. Since the landmark approval of trastuzumab in 1998,

targeted therapies that include monoclonal antibodies, tyrosine kinase inhibitors, and PARP inhibitors have been approved for metastatic breast cancer[49]. There are >80 ongoing targeted therapy-based clinical studies. However, the majority of agents in Phase II and III clinical trials assess secondary indications for previously approved therapeutic agents. Although targeted therapies can improve overall survival, few options exist for metastatic cancer and curative outcomes are negligible. Metastatic disease remains a major cancer treatment challenge that warrants a more specific drug discovery approach.

As heterogeneous populations, tumor cells vary significantly in gene expression patterns, differentiation status, and malignant potential. Genetic alterations and tumor-microenvironment interactions affect both metastatic propensity and organ tropism[50]. Metastatic organotropism represents an innovative antimetastatic target. Massagué and colleagues revolutionized the field of metastasis research by establishing the gene signatures associated with organotropic metastatic breast cancers[41,42,43]. The discovery that psammaplins selectively suppressed bone metastatic breast cancer cells opens a new arena to explore psammaplins' antitumor activities. Given the fact that a number of HDAC inhibitors are in clinical use for cancer, the next stage will be evaluating the potential of HDAC inhibitors for metastatic disease.

4. Materials and Methods

4.1. General Experimental Procedures

Routine procedures for natural product chemistry are the same as those previously described[51].

4.2. Sponge Material, Extract Preparation, and Bioassay-Guided Isolation

The sponge material was part of the NCI Open Repository Collection. Voucher specimens of *Dendrilla lacunosa* were placed on file with the Department of Invertebrate Zoology, National Museum of Natural History, Smithsonian Institution, Washington, DC. After freezing at −20 °C, the *D. lacunosa* sponge sample was ground in a meat grinder, extracted with water, the residual sample lyophilized and extracted with 50% MeOH in CH_2Cl_2[52]. The solvents were later removed under vacuum and the extract sample stored at −20 °C (NCI repository, Frederick Cancer Research and Development Center, Frederick, MD).

The *D. lacunosa* extract activated HIF-1 in a T47D cell-based reporter assay (3.56-fold at 10 μg mL^{-1}). A sample of 2.6 g was suspended in 50% MeOH in CH_2Cl_2, filtered to remove residue, and separated into eight fractions by Sephadex LH-20 column (eluted with CH_2Cl_2/MeOH, 50:50). The sixth fraction (HIF-1 activation by 2.97-fold, 1.0 μg mL^{-1}, 285 mg) was separated by a semi-preparative HPLC [Luna 5 μm, C18(2) 100 Å, 250 × 10.0 mm, isocratic 63% MeOH in H_2O, 4.0 mL min^{-1}], to produce psammaplin E (**1**, 0.8 mg, 0.03% yield, t_R 6.1 min), (*E,Z*)-psammaplin A (**2**, 1.8 mg, , 0.07% yield, t_R 10.3 min), (*E,E*)-psammaplin K (**3**, 20 mg, , 0.76% yield, t_R 11.3 min)

and (*E,E*)-psammaplin A (**4**, 155 mg, 5.92% yield, t_R 14.3 min). The MeOH eluate from HPLC column was purified by semi-preparative HPLC [Luna 5 μm, C18(2) 100 Å, 250 × 10.0 mm, isocratic 70% MeOH in 0.1%TFA/H_2O, 4.0 mL min^{-1}], to afford bisaprasin (**5**, 6.7 mg, 0.25% yield, t_R 18.2 min).

4.3. Structural Data

psammaplin E (1): oil, positive ion ESI-MS, *m/z* 479.0/481.0 [M + H]$^+$, *m/z* 501.0/503.0 [M + Na]$^+$; ^{1}H NMR (CDCl$_3$, 400 MHz): δ 7.37 (1H, d, *J* = 2.0 Hz, H-9), 7.08 (1H, dd, *J* = 8.0, 2.0 Hz, H-13), 6.77 (1H, d, *J* = 8.0 Hz, H-12), 3.80 (2H, s, H-7), 3.56 (4H, m, H-3,3'), 2.86 (4H, t, *J* = 6.8 Hz, H-2,2')[53].

(*E,Z*)-psammaplin A (2): gum, positive ion ESI-MS, *m/z* 663.0/665.0/667.0 [M + H]$^+$, *m/z* 684.9/686.9/688.9 [M + Na]$^+$; ^{1}H NMR (CD$_3$OD, 400 MHz): δ 7.37 (1H, d, *J* = 2.0 Hz, H-9), 7.32 (1H, d, *J* = 2.0 Hz, H-9'), 7.07 (1H, dd, *J* = 8.0, 2.0 Hz, H-13'), 7.02 (1H, dd, *J* = 8.0, 2.0 Hz, H-13), 6.79 (1H, d, *J* = 8.0 Hz, H-12), 6.77 (1H, d, *J* = 8.0 Hz, H-12'), 3.80 (2H, s, H-7), 3.59 (2H, s, H-7'), 3.52 (2H, t, *J* = 6.8 Hz, H-3), 3.50 (2H, t, *J* = 6.8 Hz, H-3'), 2.79 (2H, t, *J* = 7.0 Hz, H-2), 2.72 (2H, t, J = 7.0 Hz, H-2'); ^{13}C NMR (CD$_3$OD, 100 MHz): δ 164.5 (C-5'), 163.0 (C-5), 152.9 (C-6'), 152.4 (C-6), 151.7 (C-11) 151.4 (C-11'), 133.1 (C-9, 9'), 129.1 (C-13'), 129.0 (C-13), 128.9 (C-8), 128.7 (C-8'), 115.8 (C-12) 115.7 (C-12'), 109.4 (C-10), 109.1 (C-10'), 38.2 (C-3'), 37.9 (C-3), 37.0 (C-2, 2'), 36.8 (C-7'), 27.3 (C-7)[54].

(*E,E*)-psammaplin K (3): gum, positive ion ESI-MS, *m/z* 679.0/681.0/683.0 [M + H]$^+$, *m/z* 700.9/702.9/704.9 [M + Na]$^+$; ^{1}H NMR (CDCl$_3$, 400 MHz): δ 7.36 (1H, br s, H-9), 7.06 (1H, d, *J* = 7.2 Hz, H-13), 6.85 (1H, s, H-9'), 6.75 (1H, d, *J* = 8.0 Hz, H-12),

6.71 (1H, s, H-13'), 3.79 (2H, s, H-7'), 3.73 (2H, s, H-7), 3.51 (4H, t, $J = 6.8$ Hz, H-3, 3'), 2.80 (4H, t, $J = 6.8$ Hz, H-2, 2'); ^{13}C NMR (CDCl$_3$, 100 MHz): δ 164.5 (C-5, 5'), 152.3 (C-6), 151.7 (C-11, 6'), 145.7(C-12'), 141.1 (C-11'), 133.1(C-9), 129.2 (C-13), 129.0 (C-8, 8'), 123.4 (C-9'), 115.6 (C-12), 115.0 (C-13'), 109.1 (C-10, 10'), 38.2 (C-3, 3'), 37.1 (C-2, 2'), 27.5 (C-7'), 27.3 (C-7)[55].

(**E,E**)-**psammaplin A** (**4**): white powder, positive ion ESI-MS, *m/z* 663.0/665.0/667.0 [M + H]$^+$, *m/z* 684.9/686.9/688.9 [M + Na]$^+$; ^{1}H NMR (CD$_3$OD, 400 MHz): δ 7.36 (2H, d, $J = 2.0$ Hz, H-9, 9'), 7.06 (2H, dd, $J = 8.4$, 2.0 Hz, H-13, 13'), 6.75 (2H, d, $J = 8.4$ Hz, H-12, 12'), 3.79 (4H, s, H-7, 7'), 3.51 (4H, t, $J = 6.8$ Hz, H-3, 3'), 2.79 (4H, t, $J = 6.8$ Hz, H-2, 2'); ^{13}C NMR (CD$_3$OD, 100 MHz): δ 164.5 (C-5, 5'), 152.3 (C-6, 6'), 151.7 (C-11, 11'), 133.1 (C-9, 9'), 129.2 (C-13, 13'), 129.0 (C-8, 8'), 115.6 (C-12, 12'), 109.1 (C-10, 10'), 38.2 (C-3, 3'), 37.1 (C-2, 2'), 27.3 (C-7, 7')[55].

Bisaprasin (**5**): gum, negative ion ESI-MS, *m/z* 660.9/661.9/662.9 [M – 2H]$^{2-}$; ^{1}H NMR (CD$_3$OD, 400 MHz): δ 7.42 (2H, br s, H-9'', 9'''), 7.37 (2H, br s, H-9, 9'), 7.06 (4H, m, H-13, 13', 13'', 13'''), 6.77 (1H, m, H-12, 12'), 3.85 (4H, s, H-7'',7''), 3.79 (4H, s, H-7, 7'), 3.52 (8H, m, H-3, 3', 3'', 3'''), 2.79 (8H, m, H-2, 2', 2'', 2'''); ^{13}C NMR (CD$_3$OD, 100 MHz): δ 164.5 (C-5, 5', 5'', 5'''), 152.3 (C-11, 11'), 151.7 (C-6,6'), 151.6 (C-6'',6'''), 149.2 (C-11'', 11'''), 133.1 (C-9, 9'), 132.6 (C-9'', 9'''), 131.2 (C-13, 13'), 129.7 (C-8), 129.2 (C-8'), 129.0 (C-13'', 13'''), 127.2 (C-8'', 8''), 115.7 (C-12, 12'), 111.6 (C-12'', 12'''), 109.1 (C-10, 10', 10'', 10'''), 38.2 (C-3, 3', 3'', 3'''), 37.1 (C-2, 2', 2'', 2'''), 27.4 (C-7'', 7'''), 27.3 (C-7, 7')[55,56].

4.4. T47D Cell-Based Reporter Assay

Human breast cancer T47D cells (ATCC, Manassas, VA) were maintained in DMEM/F12 medium with L-glutamine (Corning, Corning, NY), supplemented with 10% (v/v) fetal bovine serum (FBS, Hyclone, Logan, Utah), 50 units mL^{-1} penicillin and 50 $\mu g\ mL^{-1}$ streptomycin (Thermo Fisher Scientific, Waltham, MA). To monitor HIF-1 activity, T47D cells were transfected with the pHRE3-TK-Luc construct and the cell-based luciferase reporter assay performed as described[35]. Cells were exposed to test compounds in the absence (pHRE-luc) and presence (pHRE-luc, 1,10-phen) of 1,10-phenanthroline (10 μM), or hypoxic conditions (1% O_2: 5% CO_2: 94% N_2) (pHRE-luc, Hypoxia) for 16 h. For the control cell-based reporter assay, T47D cells were transfected with the pGL3-control construct (Promega, Madison, WI), exposed to test compounds for 16 h, and the luciferase reporter assay performed as described[35]. Unless specified, all compounds were purchased from Sigma (St. Louis, MO).

4.5. MDA-MB-435 Cell-Based HDAC Assay

Human melanoma MDA-MB-435 cells were maintained in RPMI 1640 medium supplemented with 10% FBS, 100 units mL^{-1} penicillin and 100 $\mu g\ mL^{-1}$ streptomycin. Exponentially grown cells were seeded at the density of 5000 cells/well into 96-well plates (Corning, Corning, NY) and incubated overnight. Compounds dissolved in DMSO were added to achieve the specified final concentrations (total volume: 100 μL, DMSO: 0.5%). The incubation continued for 30 min at 37 °C and the HDAC activity determined using a commercial luminescent assay (HDAC-Glo™, Promega Corp, Madison, WI) following manufacturer's instructions. The HDAC inhibitors trichostatin A (TSA, 1 nM)

and SAHA (100nM) were used as positive controls and the data presented as percentage inhibition of the solvent control.

4.6. Quantitative Real-Time RT-PCR and ELISA Assay

The effects of test samples on HIF-1 target gene expression were assessed in T47D cells. To determine the levels of CDKN1A and VEGF mRNA, quantitative real-time RT-PCR was performed as described: 1) cell plating, compound treatment, and total RNA extraction[57]; and 2) first strand cDNA synthesis, gene-specific primer sequences, quantitative real time PCR, and data analysis[58]. To determine the levels of cellular and secreted VEGF proteins, T47D cells were exposed to compounds as described[58], the levels of VEGF proteins in the conditioned medium and cell lysate samples determined by ELISA[35], the amount of proteins in the cell lysate samples quantified using a micro BCA assay kit (Thermo Fisher Scientific, Rockford, IL), and the levels of VEGF proteins normalized to that of cellular proteins.

4.7. Cell Proliferation/Viability and Clonogenic Survival Assays

Human breast cancer T47D, MDA-MB-231, and the MDA-MB-231-derived subclones BoM1833, LM4175, and BrM-2a (J. Massagué, Memorial Sloan Kettering Cancer Center, New York, NY) were maintained in RPMI 1640 medium supplemented with 10% FBS, 50 units mL^{-1} penicillin and 50 μg mL^{-1} streptomycin. The cell proliferation/viability assay (48 h exposure) was performed as described[59]. Cell viability was determined by the sulforhodamine B method and the data presented as '% Inhibition' of the media control.

For the clonogenic assay, exponentially grown cells were seeded at the density of 1,000 cells/well into 6-well plates (Cellstar®, Greiner Bio-One GmbH, Austria) and incubated at 37° C for 4 h to allow the cells to adhere. Compound addition was similar as above. After 24 h, the compound-containing conditioned media were replaced with fresh RPMI 1640 medium containing FBS (10%) and P/S. The incubation continued for another 14 days with a change of medium every 5 days, the cells were fixed with methanol and stained with crystal violet (1 mg mL^{-1} in 20% ethanol), and the images were acquired with a Kodak digital camera.

4.8. 3D Tumor Cell Invasion Assay

A commercial kit (Cultrex® 3D Spheroid Cell Invasion Assay) was used to perform this assay, following the manufacturer's instructions (Trevigen, Gaithersburg, MD).

4.9. Statistic Analysis

Data comparison was performed with one-way ANOVA followed by Bonferroni post hoc analyses using GraphPad Prism 6. Differences between datasets were considered statistically significant when $p < 0.05$.

LIST OF REFERENCES

1. Ma, J., & Jemal, A. (2013). Breast cancer statistics. In *Breast Cancer Metastasis and Drug Resistance* (pp. 1-18). Springer New York.
2. Key, T. J., Verkasalo, P. K., & Banks, E. (2001). Epidemiology of breast cancer. *The lancet oncology*, *2*(3), 133-140.
3. Hanahan, D., & Weinberg, R. A. (2000). The hallmarks of cancer. *cell*, *100*(1), 57-70.
4. American Cancer Society (2017). Breast Cancer Treatment. Retrieved April 6, 2017, from https://www.cancer.org/cancer/breast-cancer/treatment.html
5. Gonzalez-Angulo, A. M., Morales-Vasquez, F., & Hortobagyi, G. N. (2007). Overview of resistance to systemic therapy in patients with breast cancer. In *Breast Cancer Chemosensitivity* (pp. 1-22). Springer New York.
6. Moh, M. C., & Shen, S. (2009). The roles of cell adhesion molecules in tumor suppression and cell migration: A new paradox. *Cell Adhesion & Migration*, *3*(4), 334–336.
7. Stopeck, A. T., Lipton, A., Body, J. J., Steger, G. G., Tonkin, K., De Boer, R. H., ... & Fan, M. (2010). Denosumab compared with zoledronic acid for the treatment of bone metastases in patients with advanced breast cancer: a randomized, double-blind study. *Journal of Clinical Oncology*, *28*(35), 5132-5139.
8. Weil, R. J., Palmieri, D. C., Bronder, J. L., Stark, A. M., & Steeg, P. S. (2005). Breast cancer metastasis to the central nervous system. *The American journal of pathology*, *167*(4), 913-920.
9. Mottamal, M., Zheng, S., Huang, T., & Wang, G. (2015). Histone Deacetylase Inhibitors in Clinical Studies as Templates for New Anticancer Agents. *Molecules, 20*(3), 3898-3941. doi:10.3390/molecules20033898
10. Nelson, D. L., Nelson, D. L., Lehninger, A. L., & Cox, M. M. (2008). *Lehninger Principles of Biochemistry*. New York: W.H. Freeman.
11. Ruijter, A. J., Gennip, A. H., Caron, H. N., Kemp, S., & Kuilenburg, A. B. (2003). Histone deacetylases (HDACs): Characterization of the classical HDAC family. *Biochem. J. Biochemical Journal, 370*(3), 737-749. doi:10.1042/bj20021321
12. Ahmadzadeh, A., Khodadi, E., Shahjahani, M., Bertacchini, J., Vosoughi, T., & Saki, N. (2015). The Role of HDACs as Leukemia Therapy Targets using HDI. *International Journal of Hematology-Oncology and Stem Cell Research*, *9*(4), 203–214
13. Bolden, J. E., Shi, W., Jankowski, K., Kan, C.-Y., Cluse, L., Martin, B. P., … Johnstone, R. W. (2013). HDAC inhibitors induce tumor-cell-selective pro-apoptotic transcriptional responses. *Cell Death & Disease*, *4*(2), e519–. http://doi.org/10.1038/cddis.2013.9
14. Zhang, Z. (2004). HDAC6 Expression Is Correlated with Better Survival in Breast Cancer. *Clinical Cancer Research, 10*(20), 6962-6968. doi:10.1158/1078-0432.ccr-04-0455
15. Butler, L. M., Zhou, X., Xu, W.-S., Scher, H. I., Rifkind, R. A., Marks, P. A., & Richon, V. M. (2002). The histone deacetylase inhibitor SAHA arrests cancer cell growth, up-regulates thioredoxin-binding protein-2, and down-regulates thioredoxin. *Proceedings*

of the National Academy of Sciences of the United States of America, 99(18), 11700–11705. http://doi.org/10.1073/pnas.182372299

16. Belvedere, S., Witter, D. J., Yan, J., Secrist, J. P., Richon, V., & Miller, T. A. (2007). Aminosuberoyl hydroxamic acids (ASHAs): A potent new class of HDAC inhibitors. *Bioorganic & Medicinal Chemistry Letters, 17*(14), 3969-3971. doi:10.1016/j.bmcl.2007.04.089

17. Vorinostat: Medline Plus Drug Information. (2009, February 1). Retrieved May 5, 2016, from https://www.nlm.nih.gov/medlineplus/druginfo/meds/a607050.html

18. Gao, M., Chen, G., Wang, H., Xie, B., Hu, L., Kong, Y., . . . Shi, J. (2014). Therapeutic potential and functional interaction of carfilzomib and vorinostat in T-cell leukemia/lymphoma. *Oncotarget*. doi:10.18632/oncotarget.8667

19. Vorinostat (SAHA, MK0683). (2013). Retrieved May 06, 2016, from http://www.selleckchem.com/products/Vorinostat-saha.html

20. Praseetha, S., Bandaru, S., Nayarisseri, A., & Sureshkumar, S. (2016). Pharmacological Analysis of Vorinostat Analogues as Potential Anti-tumor Agents Targeting Human Histone Deacetylases: An Epigenetic Treatment Stratagem for Cancers. *Asian Pacific Journal of Cancer Prevention*. http://dx.doi.org/10.7314/APJCP.2016.17.3.157z

21. Marks, P. A. (2007). Discovery and development of SAHA as an anticancer agent. *Oncogene, 26*(9), 1351-1356. doi:10.1038/sj.onc.1210204

22. Romidepsin Injection: Medline Plus Drug Information. (2009, February 1). Retrieved May 5, 2016, from https://www.nlm.nih.gov/medlineplus/druginfo/meds/a610005.html

23. Li, L., Zhang, P., Cai, P., & Li, Z. (2016). Original article: Histone deacetylase inhibitor, Romidepsin (FK228) inhibits endometrial cancer cell growth through augmentation of p53-p21 pathway. *Biomedicine & Pharmacotherapy*, doi:10.1016/j.biopha.2016.04.053

24. Romidepsin (FK228, Depsipeptide). (2013). Retrieved May 06, 2016, from http://www.selleckchem.com/products/Romidepsin-FK228.html

25. Patel PM, Patel HH, Roth DM (2011) General Anesthetics and Therapeutic Gases. Chapter 19 in Goodman and Gilman's The Pharmacological Basis of Therapeutics, 12th Edition, Brunton LL, Chabner BA, Knollman BC, Ed., pp. 527-564. McGraw Hill Medical.

26. Michiels C (2004) Physiological and pathological responses to hypoxia. *Am J Pathol* 164, 1875-1882.

27. Nallamshetty S, Chan SY, Loscalzo J (2013) Hypoxia: a master regulator of microRNA biogenesis and activity. *Free Radic Biol Med* 64, 20-30.

28. Span PN, Bussink J (2015) Biology of hypoxia. *Semin Nucl Med* 45, 101-109.

29. Semenza GL (2014) Oxygen sensing, hypoxia-inducible factors, and disease pathophysiology. *Annu Rev Pathol* 9, 47-71.

30. Keith B, Johnson RS, Simon MC (2012) HIF1α and HIF2α: sibling rivalry in hypoxic tumour growth and progression. *Nat Rev Cancer* 12, 9-22.

31. Semenza GL (2012) Hypoxia-inducible factors: mediators of cancer progression and targets for cancer therapy. *Trends Pharmacol Sci* 33, 207-214.

32. Bouchie A (2013) First-in-class anemia drug takes aim at Amgen's dominion. *Nat Biotechnol* 31, 948-949.
33. Forristal CE, Levesque JP (2014) Targeting the hypoxia-sensing pathway in clinical hematology. *Stem Cells Transl Med* 3, 135-140.
34. Rabinowitz MH (2013) Inhibition of hypoxia-inducible factor prolyl hydroxylase domain oxygen sensors: tricking the body into mounting orchestrated survival and repair responses. *J Med Chem* 56, 9369-9402.
35. Hodges TW, Hossain CF, Kim YP, Zhou YD, Nagle DG. (2004). J Nat Prod. 67:767–771.
36. Hong S, Shin Y, Jung M, Ha MW, Park Y, Lee YJ, Shin J, Oh KB, Lee SK, Park HG (2015) Efficient synthesis and biological activity of Psammaplin A and its analogues as antitumor agents. *Eur J Med Chem* 96, 218-230.
37. Kim TH, Kim HS, Kang YJ, Yoon S, Lee J, Choi WS, Jung JH, Kim HS (2015) Psammaplin A induces Sirtuin 1-dependent autophagic cell death in doxorubicin-resistant MCF-7/adr human breast cancer cells and xenografts. *Biochim Biophys Acta* 1850, 401-410.
38. Ahn MY, Jung JH, Na YJ, Kim HS (2008) A natural histone deacetylase inhibitor, Psammaplin A, induces cell cycle arrest and apoptosis in human endometrial cancer cells. *Gynecol Oncol* 108, 27-33.
39. Mora FD, Jones DK, Desai PV, Patny A, Avery MA, Feller DR, Smillie T, Zhou YD, Nagle DG (2006) Bioassay for the identification of natural product-based activators of peroxisome proliferator-activated receptor-gamma (PPARgamma): the marine sponge metabolite psammaplin A activates PPARgamma and induces apoptosis in human breast tumor cells. *J Nat Prod* 69, 547-552.
40. American Cancer Society (2012) Breast Cancer, Facts & Figures 2011-2012 http://www.cancer.org/acs/groups/content/@epidemiologysurveilance/documents/document/acspc-030975.pdf
41. Kang Y, Siegel PM, Shu W, Drobnjak M, Kakonen SM, Cordón-Cardo C, Guise TA, Massagué J (2003) A multigenic program mediating breast cancer metastasis to bone. Cancer Cell 3, 537-549.
42. Minn AJ, Gupta GP, Siegel PM, Bos PD, Shu W, Giri DD, Viale A, Olshen AB, Gerald WL, Massagué J (2005) Genes that mediate breast cancer metastasis to lung. Nature, 436, 518-524.
43. Bos PD, Zhang XH, Nadal C, Shu W, Gomis RR, Nguyen DX, Minn AJ, van de Vijver MJ, Gerald WL, Foekens JA, Massagué J (2009) Genes that mediate breast cancer metastasis to the brain. Nature, 459, 1005-1009
44. Nagle, D.G.; Zhou, Y.-D. "Natural product-derived small molecule activators of hypoxia-Inducible Factor-1 (HIF-1)" Curr. Pharm. Design 2006, 12, 2673–2688.
45. García J, Franci G, Pereira R, Benedetti R, Nebbioso A, Rodríguez-Barrios F, Gronemeyer H, Altucci L, de Lera AR (2011) Epigenetic profiling of the antitumor natural product psammaplin A and its analogues. Bioorg Med Chem 19, 3637-3649.
46. Ferrara N, Adamis AP (2016) Ten years of anti-vascular endothelial growth factor therapy. Nat Rev Drug Discov. 15(6):385-403.
47. Cancer Research UK (2011) CancerStats, Cancer Worldwide http://publications.cancerresearchuk.org/downloads/product/CS_CS_WORLD.pdf.

48. Sethi N, Kang Y (2011) Unravelling the complexity of metastasis - molecular understanding and targeted therapies. *Nature Reviews Cancer*, 11, 735-748.

49. Wan L, Pantel K, Kang Y (2013) Tumor metastasis: moving new biological insights into the clinic. *Nature Medicine*, 19, 1450-1464.

50. Nguyen DX, Massagué J (2007) Genetic determinants of cancer metastasis. *Nature Reviews Genetics*, 8, 341-352.

51. Du, L., Zhou, Y. D., & Nagle, D. G. (2013). Inducers of hypoxic response: Marine sesquiterpene quinones activate HIF-1. *Journal of natural products*, *76*(6), 1175.

52. McCloud TC. Molecules. 2010; 15:4526–4563

53. Piña, I. C., Gautschi, J. T., Wang, G. Y. S., Sanders, M. L., Schmitz, F. J., France, D., Cornell-Kennon S., Sambucetti L. C., Remiszewski S. W., Perez L. B., Bair, K. W. (2003). Psammaplins from the Sponge Pseudoceratina p urpurea: Inhibition of Both Histone Deacetylase and DNA Methyltransferase. *The Journal of organic chemistry*, *68*(10), 3866-3873.

54. Park, Y., Liu, Y., Hong, J., Lee, C. O., Cho, H., Kim, D. K., ... & Jung, J. H. (2003). New Bromotyrosine Derivatives from an Association of Two Sponges, Jaspis w ondoensis and Poecillastra w ondoensis. *Journal of natural products*, *66*(11), 1495-1498.

55. Tabudravu J.N., Eijsink V.G.H, Gooday G.W., Jaspars M., Komander D., Legg M., et al. (2002) Psammaplin A, a chitinase inhibitor isolated from the Fijian marine sponge *Aplysinella rhax*. Bioorg. Med. Chem. 10, 1123–1128

56. Rodríguez, A.D.; Akee, R.K.; Scheuer, P.J. (1987). Two bromotyrosine-cysteine derived metabolites from a sponge. *Tetrahedron Lett. 28*, 4989–4992.

57. Hossain, C. F., Kim, Y. P., Baerson, S. R., Zhang, L., Bruick, R. K., Mohammed, K. A., ... & Zhou, Y. D. (2005). Saururus cernuus lignans—Potent small molecule inhibitors of hypoxia-inducible factor-1. *Biochemical and biophysical research communications*, *333*(3), 1026-1033.

58. Zhou, Y. D., Kim, Y. P., Li, X. C., Baerson, S. R., Agarwal, A. K., Hodges, T. W., ... & Nagle, D. G. (2004). Hypoxia-inducible factor-1 activation by (−)-epicatechin gallate: potential adverse effects of cancer chemoprevention with high-dose green tea extracts. *Journal of natural products*, *67*(12), 2063-2069.

59. Liu, Y., Veena, C. K., Morgan, J. B., Mohammed, K. A., Jekabsons, M. B., Nagle, D. G., & Zhou, Y. D. (2009). Methylalpinumisoflavone inhibits hypoxia-inducible factor-1 (HIF-1) activation by simultaneously targeting multiple pathways. *Journal of Biological Chemistry*, *284*(9), 5859-5868.